

INVESTIGATION ON ROTOR BLADE-WAKE INTERACTION NOISE IN DESCENT FLIGHT CONDITIONS

Panagiotis A. Vitsas and Penelope Menounou
Department of Mechanical and Aeronautical Engineering
University of Patras, Rion 26504, Patras, Greece

Abstract

Helicopter rotor Blade Wake Interaction (BWI) noise is known to be significant during take-off and level flight. Less attention has been given to descent flight conditions, where Blade Vortex Interaction (BVI) noise is dominant. The present study investigates BWI noise in descent flight conditions by analyzing acoustic and aerodynamic data from the HELISHAPE test. It is shown that BWI fluctuations (of both acoustic and blade pressure waveforms) can be categorized in two types with respect to their origin: one type is associated with impulsive BVI, while the other with blade turbulence interaction. The statistical and spectral properties of these fluctuations reinforce theories that relate BWI noise to coherent eddies present in the flow. Further, the location of the interacting vortices reveals that younger vortices do not contribute to BWI noise levels. Finally, it is shown that the blade tip shape does not significantly affect BWI noise.

1. INTRODUCTION

Helicopter rotor noise has been the field of many experimental and theoretical studies since the eighties, aiming to improve its understanding and prediction. Generally, helicopter noise can be categorized in impulsive and broadband, while the mechanisms that generate it depend strongly on the flight conditions. Impulsive rotor noise, resulting from the periodic interaction of the blade tips with vortices ingested in the rotor, is important at frequencies below 1000Hz, while the higher frequencies are dominated by broadband noise. In descent flight conditions Blade Vortex Interaction (BVI) noise, which is impulsive in nature, dominates the acoustic spectrum^{[1],[2]}, while in take-off and level flight conditions a type of broadband noise named Blade Wake Interaction (BWI) noise is usually the most important noise contributor. BWI noise was initially identified by Brooks *et al.*^[3] After a series of wind tunnel tests on model scale rotors they concluded that broadband rotor noise is generated by the interaction of the rotor blades with features of the inflow, which depend on the rotor operating conditions. Specifically, broadband noise depends on the ingestion of blade wake turbulence into the rotor, while the amount of wake ingestion controls the noise levels. Glegg^[4] tried to build a prediction model for BWI based on the assumption that the noise was generated from interactions between the blades and isotropic homogeneous turbulence contained in tip vortices. However, results indicated that the energy contained in an isolated vortex was not sufficient to account for BWI noise levels. This finding prompted Wittmer^[5] to search for other

mechanisms of turbulence production inside trailing vortices. He showed that there was significantly higher level of turbulence energy contained in the zone around a tip vortex, when it had already interacted with a blade. Glegg *et al.*^[6] modified Glegg's model accordingly and obtained noise levels in agreement with experimental data. In contrary to the above, Brezzillon *et al.*^[7] analyzing HART^[8] experimental blade pressures showed that contributions of tip vortices that have not previously interacted with a blade were comparable to contributions of vortices having already encountered a blade. A thorough analysis of HART experimental blade pressures done by Bouchet and Rahier^[9] demonstrated that BWI was not related to blade interactions with isotropic turbulence, but rather to coherent large-scale structures present in the flow. Based on the observation that BWI pressure fluctuations occur at azimuths where the blade interacts with two close tip-vortices, Bouchet suggested that BWI noise is attributed to elliptic instabilities of co-rotative vortex pairs^[10]. A numerical simulation of these instabilities by Mauffrey *et al.*^[12] in take-off flight conditions showed that the interaction of rotor blades and vortices subject to elliptical instabilities is a good candidate mechanism to explain BWI generation. At the current state of the art, the generation mechanism of BWI is still under investigation.

A variety of methods has been used for the investigation of BWI noise ranging from experiments, to numerical modeling and data analysis. The present study employs analysis of experimental data. The studies of Brezzillon *et al.*^[7] and Bouchet and Rahier^[9], to the authors' best knowledge, are the

only studies on BWI noise that have been based on acoustic and blade pressure measurements' analysis. These studies mainly focused on take-off flight conditions. The case of descent flight conditions has received less attention due to the relative smaller importance of BWI noise in the acoustic spectrum. Despite its smaller importance, it is seen in the HART acoustic spectrum results (Figure 1) that the descent case experiences the greater BWI spectrum levels compared to the other conditions. The only comment on descent flight conditions is made in the study of Brezzillon *et al.* who concluded that parallel blade vortex interactions, which generate impulsive noise in descent flight, are also sources of BWI noise. However, they did not explain all BWI pressure fluctuations and suggested that interactions with parts other than tip vortices also contribute to BWI noise.

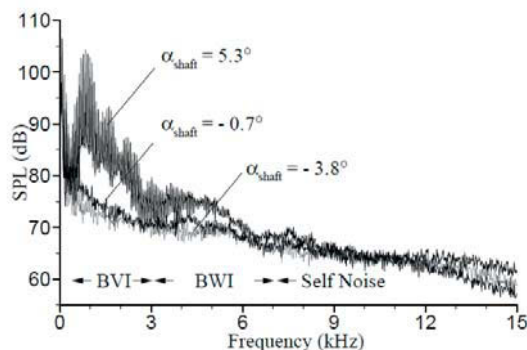


Figure 1. Noise spectra for three typical flight conditions (taken from Ref [7]).

The present study analyzes acoustic pressure and blade pressure data to examine the importance of BWI noise in descent flight conditions and to provide supporting evidence to the various suggested BWI mechanisms. Initially, a brief description of the HELISHAPE^[11] test is presented, making this the first study to use this experiment for BWI noise analysis. BWI contribution in acoustic and blade pressure data is determined using appropriate filters and the resulting BWI fluctuations are analyzed in terms of Strouhal number and fluctuation probability distribution. The agreement between acoustic and aerodynamic analysis results is examined and results are compared to those of the take-off analysis made by Bouchet *et al.* Furthermore, the localization of the dominant BWI region on the rotor disk and the position of blade pressure fluctuations are derived. The vortices, which are mainly contributing to BWI noise, are determined and their association to the suggested mechanisms is examined. Finally, the effect of blade-tip shape on BWI noise is briefly outlined.

2. EXPERIMENT DESCRIPTION

Within the framework of a major European cooperative research program on rotorcraft aerodynamics and acoustics (HELISHAPE) a parametric model rotor test was conducted in 1995. The main objectives of this experimental research were to evaluate noise reduction techniques (conceptually by variation of rotor speed, dedicated tip shapes and advanced airfoils) and to validate the partners' individual aerodynamic and aeroacoustic codes. Though the objectives did not include broadband noise studies, the microphones and blade pressure transducers used in the experiment were of high enough sampling rate to allow BWI noise analysis.

2.1. Experimental Setup and selected test cases

The HELISHAPE test is described in detail in Ref [11]. The experiment was conducted in the open test section of the German-Dutch Wind Tunnel (DNW) using the MWM test rig of DLR and a highly instrumented model of a fully articulated ECF four bladed 2.1m radius rotor equipped with blades of advanced design and two exchangeable blade tips. The one set of blade tips (7A) was of rectangular shape, the other one (7AD) of swept-back parabolic/anhedral shape. The tests covered hover, descent, climb, low speed and intermediate speed level flight. The flight condition selected for the present study was low speed descent flight, at 6° descent angle for both blade tips. These test cases were performed with a rotational tip Mach number of 0.62, an advance ratio $\mu=0.166$ (corresponding to a wind tunnel flow velocity of $U_{inf}=33$ m/sec) and a rotor operating speed of 970 rpm. The rotor thrust coefficient (C_T) was close to 0.069.

2.2. Acoustic and aerodynamic measurements

The acoustic instrumentation consisted of a linear inflow array of eleven microphones (B&K 4134) mounted on a traversing system. The microphone array's vertical position was 2.3m below the rotor hub and it moved slowly in the flow direction acquiring signals every 0.5m from 4m upstream to 2m downstream of the rotor hub. Acoustic results were thus provided on an array of 143 (13 x 11) microphone locations underneath the rotor [Figure 2(a) and (b)].

The recording of the signals was in synchronization with the rotation of the rotor shaft and the microphone signals were conditionally sampled at a rate of 2048 per revolution over a period of 30 rotor revolutions, giving a useful frequency range of about 18 kHz. For each acoustic measurement point the ensemble averaged sound pressure time histories and averaged power spectra were calculated.

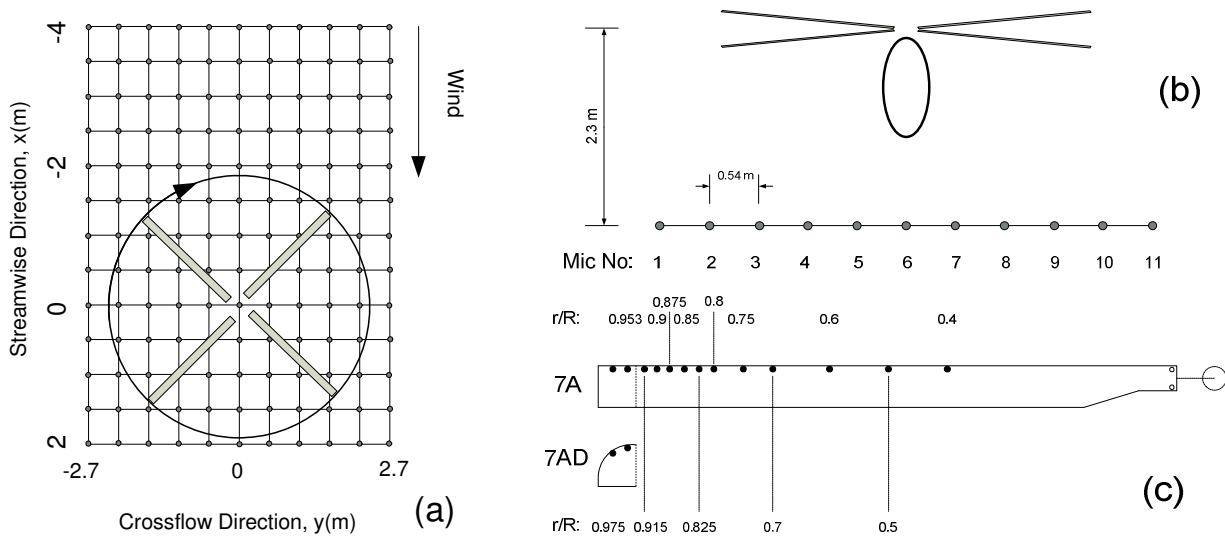


Figure 2. Experiment setup; top view (a), view from the back (b), and positions of pressure transducers on the rotor blades (c).

For the blade pressure measurements 118 absolute pressure transducers of the piezoresistive (Kulite XCD) type were distributed on all four blades to measure the chordwise pressure distribution and the radial distribution near the leading edge [Figure 2 (c)]. The blade pressure signals were acquired over 60 rotor revolutions at the same rate as microphone signals and were processed similarly.

3. ANALYSIS OF ACOUSTIC DATA

The analysis of the acoustic data will be performed for both measured acoustic pressure waveforms and spectra. The analysis aims to specify the contribution of BVI noise in the BWI spectrum region, as well as, to locate the rotor azimuth region responsible for BWI noise. Further, the acoustic data are used, for the first time, to derive certain characteristics of the wake turbulence encountered by the blades. For this study a frequency range of 0.4 kHz to 2.6 kHz (5-40bpf) is considered characteristic of BVI noise, while 2.8 kHz to 6 kHz (43-93bpf) is associated to BWI noise. The ranges are similar to those used by Brezillion *et al.*

3.1. Types of BWI acoustic pressure fluctuations

In order to isolate the BWI pressure component of the acoustic pressure waveforms, a band pass filter for the BWI frequency region of the spectrum is applied to the instantaneous acoustic

signals. Results are shown for Mic 3 / $x=-2$, which contains advancing side BVI noise and at the same time high levels of BWI noise [Figure 3 (a)]. Similar results are observed for the other advancing side microphones. The resulting BWI-filtered waveform can be seen in Figure 3 (c) for one rotor revolution (T). The signal contains both random and periodic components. Closer observation of a single blade passage [shown in Figure 3 (b)] reveals that the BWI signal consists of two defined regions. The first region contains the higher amplitude fluctuations, which have the same phase position as BVI pulses [compare Figure 3(b) and (d)]. These fluctuations will be named “*Type I fluctuations*” hereinafter. The second region contains lower amplitude fluctuations that come immediately after the strong BVI pulses and will be named “*Type II fluctuations*”.

As it will be shown later in this paper, Type I fluctuations correspond to the higher harmonics of BVI noise and are attributed to the steepness of the BVI pulses. The existence of BWI fluctuations connected to BVI impulses has also been referenced by Bouchet and Rahier^[9] as “BWI-like” fluctuations in their analysis of blade pressure waveforms. Type II fluctuations represent the actual BWI noise and, as will be shown later, are random.

As Type I fluctuations are attributed to the steepness of BVI pulses, the sensitivity of this characteristic might change their amplitude and, thus, their relative importance compared to Type II fluctuations. For the HELISHAPE data, Type I fluctuations are of higher amplitude than Type II. Type I fluctuations might be of smaller amplitude, when the BVI pulses are less steep. For all advancing side signals, Type I fluctuations come

before Type II. On the contrary, for microphones containing strong retreating side BVI pulses, Type II fluctuations tend to come before BVI pulses (Figure 4). This observation agrees with all suggested BVI mechanisms, as blades moving from upwind to downwind encounter the turbulent sections of the rotor wake before the impulsive parallel blade vortex interactions. Because retreating side BVI levels are very low, they will not be examined further in this study.

Closer observation of Figure 3(b) reveals some small-amplitude, high-frequency acoustic fluctuations on top of the BVI pulses. Judging from their phase position in the acoustic waveform, these fluctuations could be attributed to the blade interacting with turbulence in the vortex core or in the

very close vicinity around the vortex. However, spectral analysis of those fluctuations showed that they do not contribute to the BVI frequency region, as they correspond to even higher frequencies and, thus, will not be analyzed further in this study.

It should be noted that in addition to the application of the band pass filter presented above, the subtraction of the average waveform from the instantaneous waveform and application of a high pass filter was also performed in the present study as an alternate method to remove the medium frequency components^[9]. The two methods provided almost identical results. However, the second method is less accurate due to the error introduced in the average time histories from the ensemble averaging method^[13].

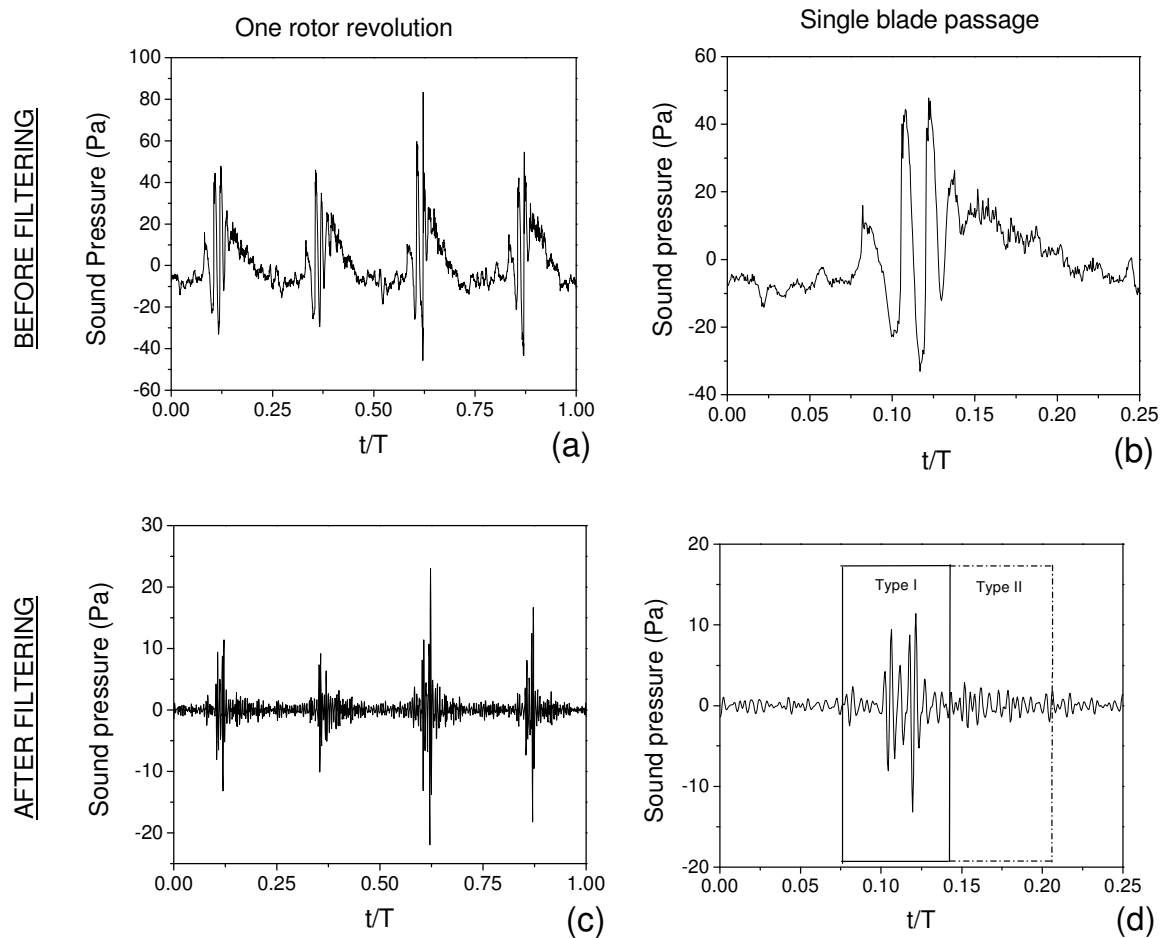


Figure 3. Instantaneous advancing side BVI acoustic signal before and after applying the BVI filter for one rotor revolution [(a),(c)] and for a single blade passage [(b),(d)]; fluctuations corresponding to the traditional BVI frequency region are subdivided into Type I and Type II fluctuations (d).

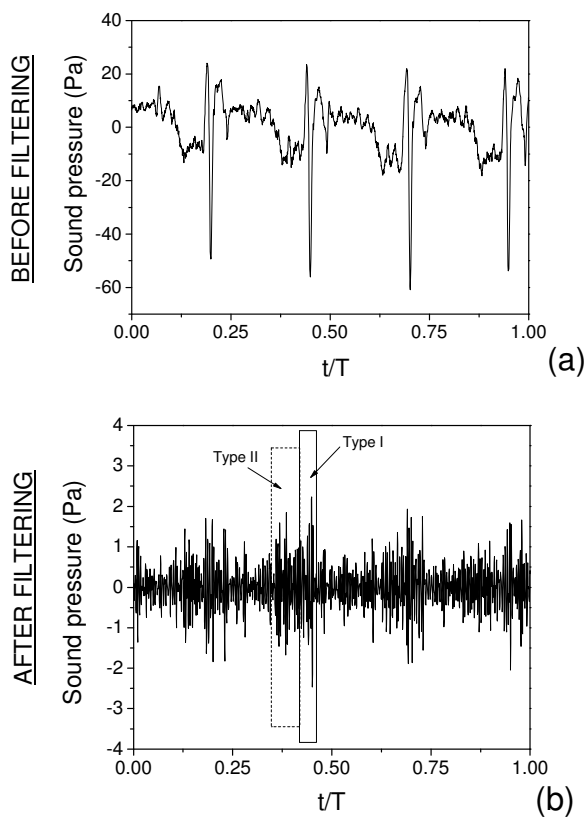


Figure 4. Instantaneous retreating side BVI acoustic signal before [a] and after [b] applying the BVI filter.

3.2. Azimuthal localization of BWI region on the rotor disk

In order to identify the azimuthal range on the rotor disk that is associated with noise in the BWI frequency region, a BVI localization scheme^[15] has been appropriately modified and applied to the BWI fluctuation waveforms. This localization scheme has been applied in the past for localization of BVI discrete pulses. It cannot be directly applied to broadband BWI noise due to the lack of discrete waveform points. The new element of the procedure presented here is how to identify the BWI broadband waveform for use with the localization scheme. First, the BWI-filtered signal is broken into four equal parts, each part corresponding to a blade passage. Overlapping of these parts reveals the general pattern of BWI fluctuations, as seen in Figure 5(a). The four different blade passage BWI fluctuations show strong consistency in terms of phase and amplitude. The average of the absolute values of these fluctuations is evaluated and compared to the average waveform of the same microphone [Figure 5(b)]. It is observed that the greater values of the average BWI fluctuations coincide with the steep BVI slopes of pulses B and C

revealing that these fluctuations are in fact the higher harmonics of BVI noise. The observation that Type I fluctuations are fully attributed to BVI noise contradicts Brezzilion's conclusion that parallel BVIs, which generate impulsive noise, are also sources of BWI noise. In other words, parallel BVIs are the sources of Type I fluctuations, but not of Type II.

BWI fluctuations of Type II [see Figure 5(b)] can be considered to be between pulses D and H of the average waveform. BVI localization procedure is applied for pulses A, D and H. Azimuth region between pulses A and D can be considered an estimate for the dominant parallel BVI region containing strong discrete pulses and Type I fluctuations. Azimuth region between D and H can be considered as an estimate of acoustically most significant BWI region containing Type II fluctuations. The localization method was validated by comparing the resulting BVI locations to HELISHAPE Laser Light Sheet (LLS) measurements and blade pressure measurements.

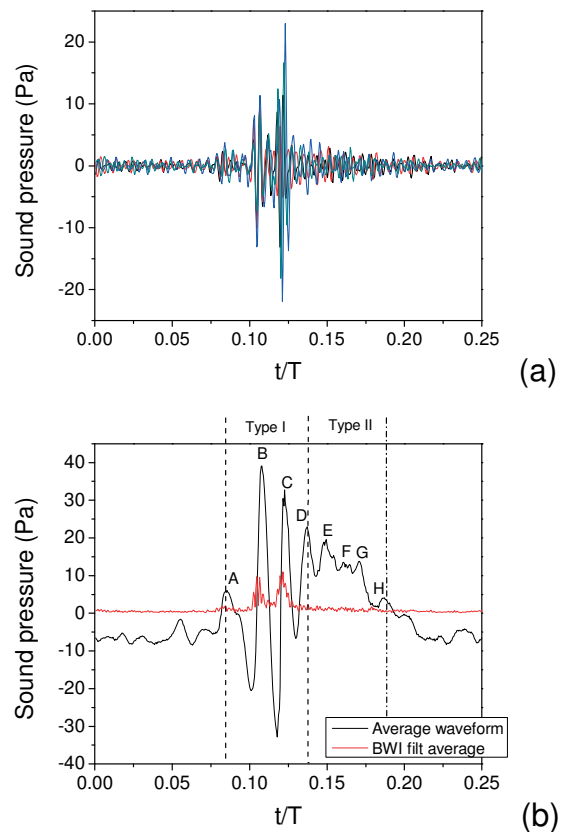


Figure 5. Pattern of BWI fluctuations revealed by overlapping all four BVI-filtered blade passages (a) and association of the average absolute fluctuations with the average acoustic pressure waveform (b).

The azimuthal ranges associated with Type I fluctuations are found to be between 50 and 85 deg. This is the typical region of parallel BVIs in descent flight conditions, which can also be derived from blade pressure measurements. The range for Type II fluctuations is set between 85 and 115 deg, which is the range that blade wake turbulence interaction mostly occurs (Figure 6). The BWI region localization result is somewhat different from Marcolini's result^[14], which placed the highest BWI levels in the first quadrant of the rotor disk. This disagreement could possibly be attributed to the microphone measuring the high amplitude Type I fluctuations due to the steep BVI pulses and attributing them to BWI noise.

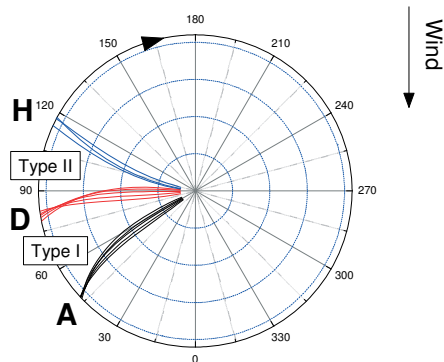


Figure 6: Azimuthal ranges on the rotor disk associated with Type I and Type II fluctuations.

3.3. Statistical and spectral properties of BWI acoustic pressure fluctuations

The difference in the physical origin of the two types of BWI fluctuations can also be seen by examining the statistical properties of the two regions. The windows used for the statistical analysis of the two types of BWI fluctuations are based on their azimuth range derived in the previous paragraph. The statistical distribution of the fluctuations seen in the Type I region (50 to 85 deg window) deviates significantly from Gaussian distribution [Figure 7 (a)]. On the other hand, Type II region fluctuations (85 to 115 deg window) exhibit an almost Gaussian distribution [Figure 7 (b)] revealing their random origin.

In order to examine the spectral properties of Type II fluctuations and associate them to a Struhal number, FFT was applied to the Type II fluctuations of each blade passage and the average of the four spectra was computed. The average spectrum of the

Type II fluctuations is plotted in Figure 7 (c) versus non-dimensional frequencies, namely Struhal number (S_t):

$$(1) \quad S_t = fc / U$$

where f denotes the frequency, c the blade chord and U the chordwise convection speed with respect to the blade section.

Figure 7 (c) shows that the Type II fluctuations' spectrum exhibits a local maximum around $S_t = 2.5$. This is the same value that has been derived by blade pressure analysis in take off flight conditions^[9] and has been related to coherent structures encountered by the blade during blade vortex interaction. For the first time it is pointed out in the present study that the acoustic fluctuations and coherent structures of the flow show similarities. This analysis enforces Bouchet and Rahier's suggestion that BWI noise is associated with coherent eddies of the wake flow.

Statistical and spectral results were also confirmed by analyzing acoustic waveforms of other microphones containing high BWI levels.

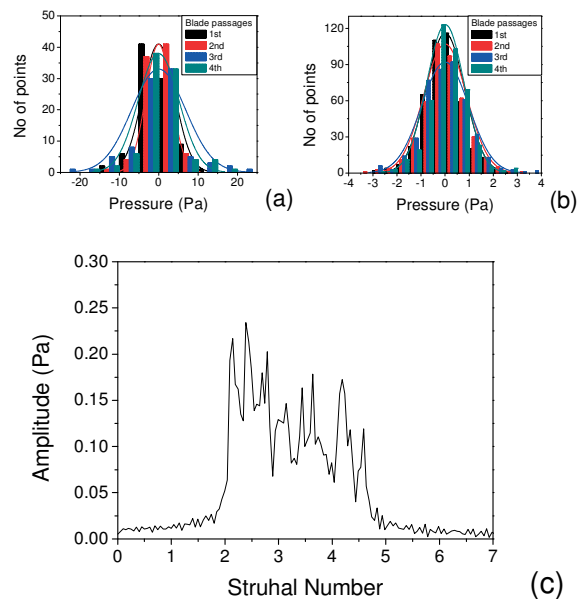


Figure 7: Statistical distribution of Type I (a) and Type II (b) fluctuations and average spectrum of Type II fluctuations (c). (Mic 3 / $x=-2$)

3.4. Contribution of BVI noise in the BWI spectrum region

The contribution of BVI noise in the BWI spectrum region analyzed in the previous sections can also be observed in the acoustic spectra.

Acoustic data from the HELISHAPE test include both average and coherent power spectra. Average power spectra contain energy of both the periodic and random parts of the signal, while in the

coherent spectra (power spectra of the average time history) the contribution of the random phenomena has been removed [Figure 8 (a)]. Ideally average spectra BWI levels contain contributions of Type I and Type II fluctuations, while coherent spectra contain only Type I fluctuations. The logarithmic subtraction of the coherent from the average spectra gives an estimate of Type II levels only and will be referred to as dBWI hereinafter.

Averaged spectra BWI levels and dBWI spectra levels are plotted for all array microphones in the contours of Figure 8 (b) and (c), respectively. The amplitude of the spectrum dBWI is slightly decreased in the order of 2-3dB compared to the average spectrum values, while the directivity and maximum region do not change. This result agrees with the error estimation of Ref [3] and can be considered a more accurate representation of BWI noise levels. However average spectrum levels are a good approximation when this procedure is not feasible.

It is recommended that a similar analysis should be made using spectra from conditionally averaged waveforms which are shown to be less affected by the averaging method.

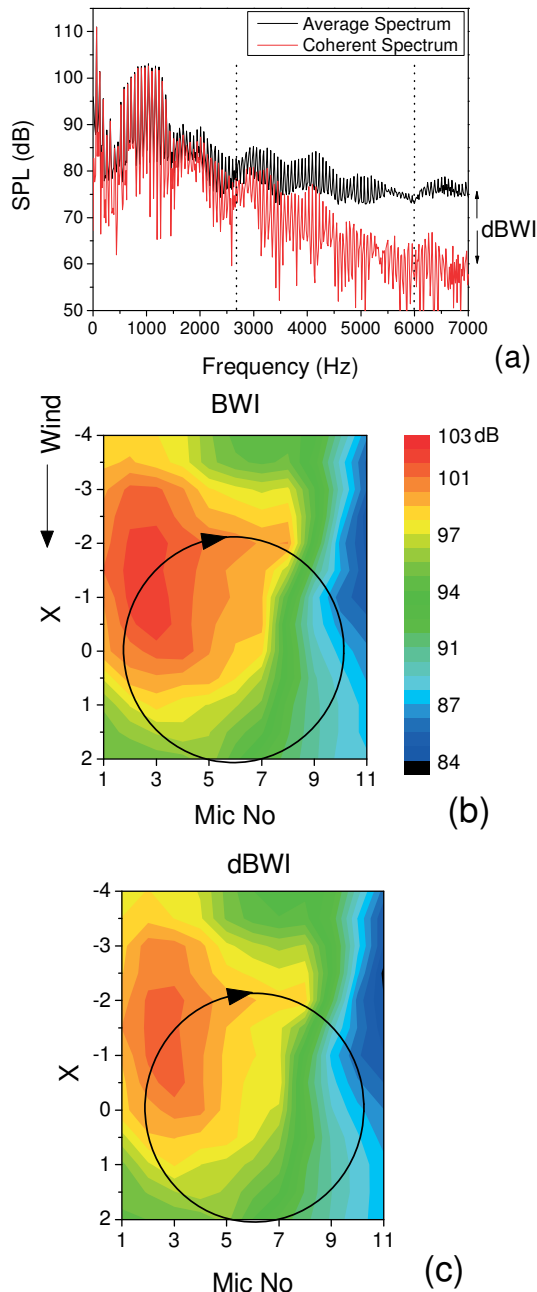


Figure 8. Average and coherent spectra of Mic 3/x=-2 (a), BWI noise contour based on average spectrum (b), dBWI contour (c).

4. ANALYSIS OF AERODYNAMIC DATA

A similar analysis to that of acoustic pressure data is performed for the blade pressure signals. The data employed are the instantaneous and the averaged blade pressure waveforms measured at 2% chord. Results regarding BWI locations and turbulence characteristics are compared to and combined with the acoustic results.

4.1. Definition of BWI region on rotor disk and of interacting vortices

In order to locate in span and azimuth the pressure fluctuations regarded as potential BWI noise sources, BWI frequency band-pass filters are applied to the differential pressures (ΔC_p) of the leading edge sensors at 2% chord. The plots of BWI and BVI fluctuations on the rotor disk are shown in Figure 9. The region shown ranges from 0.6R to the outboard region, which is known to be the acoustically significant part of the rotor disk.

Figure 9 (a) shows that BWI pressure fluctuations can be found at many regions around the rotor disk. Significant congestion of fluctuations can be seen roughly on three sections of the rotor disk: (i) on the advancing side, (ii) on the downwind retreating side and (iii) at the further downwind end of the rotor disk. Not all of these fluctuations are responsible for BWI noise. Again, Type I and Type II fluctuations will be distinguished with respect to their origin being impulsive blade-vortex interaction or blade-turbulence interaction. In order to distinguish

between the different types of fluctuations shown in Figure 9 (a), they will be compared against fluctuations resulting from the filtering of averaged blade pressure waveforms, which are therefore exclusively Type I fluctuations attributed to the higher harmonics of BVI pulses [shown in Figure 9 (c)].

The region of fluctuations at the further end of downwind side (around azimuth of 0 degrees) is attributed to (i) measurement discontinuities due to one-rotor revolution recordings and (ii) to interaction of the blades with the upper fuselage wake due to its angle to the free flow. The retreating side region shows significant content of BWI fluctuations. However, the acoustic fluctuations in the retreating side region are very small compared to those at the advancing side, as it has been seen in the acoustic analysis section. In the upwind retreating side, the blade pressure fluctuations are of smaller acoustic importance, possibly, due to the decreased blade turbulence interaction velocity and will not be further investigated in this study. In the downwind retreating side, the high content of BWI fluctuations, which coincides with blade vortex interaction locations around the azimuth of 300 degrees are Type I retreating side fluctuations and are partially seen in Figure 9 (c).

The acoustically most important BWI fluctuations are the ones found on the advancing side of the rotor. The fluctuations seen in Figure 9 (a) on the advancing side region (from about 50 to 85 degrees) coincide with parallel BVIs seen in Figure 9 (b) and are therefore Type I BWI fluctuations. Smaller fluctuations seen in the region of 85 to 120 deg can be characterized as Type II fluctuations as are they are only present in the instantaneous plot [compare Figure 9 (a) and (c)]. These fluctuations seem to be small in amplitude but they are exactly in the region, which has been found from the acoustic analysis to be the most significant for BWI noise. Combination of the acoustic and aerodynamic localization results sets the Type II fluctuations region (and, thus, the acoustically most important BWI region) to be between $0.85R$ at 85 deg and $0.62R$ at 115 deg azimuth.

In order to determine the exact vortices found in that region rotor wake geometry charts^[16] are used. Figure 10 shows the blade vortex interaction locations for a flight condition case very close to that examined in this study. The vortices which correspond to the derived BWI region are shown to be enclosed in the red dashed line.

In terms of interaction angle, the interactions shown in the circled BWI region are oblique, almost perpendicular. This agrees with existing knowledge for this type of noise source. A closer look into Figure 10 shows that BWI noise is mostly attributed to the interaction of blade 1 with two vortices that come from the preceding blades: blade 3 vortex having an age of 150-160deg and blade 2 vortex having an age of 230 to 235 deg.

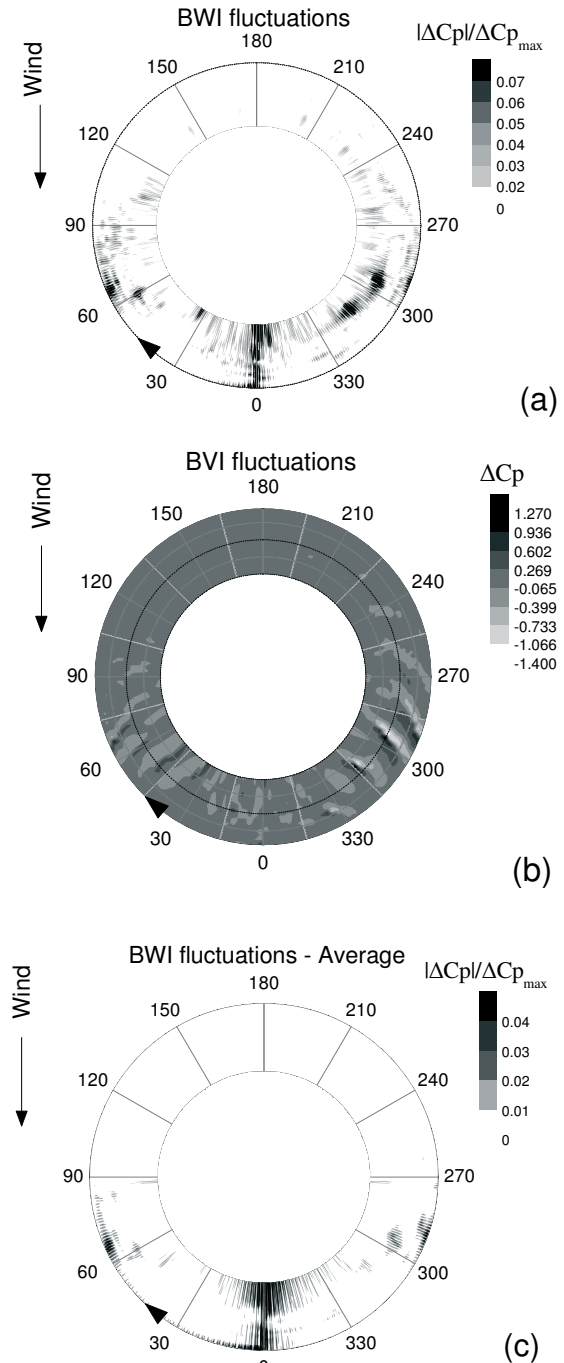


Figure 9: BWI blade pressure fluctuations on rotor disk from instantaneous signals (a), BVI blade pressure fluctuations from instantaneous signals (b) and BWI blade pressure fluctuations from average signals (c)

These interaction locations are shown in Figure 10 as “1,3” and “1,2” respectively. Both vortices have already encountered one or more interactions, while blade 4 vortex, which is generated from exactly the previous blade and has an age of less than 80 deg, does not seem to contribute to BWI pressure fluctuations.

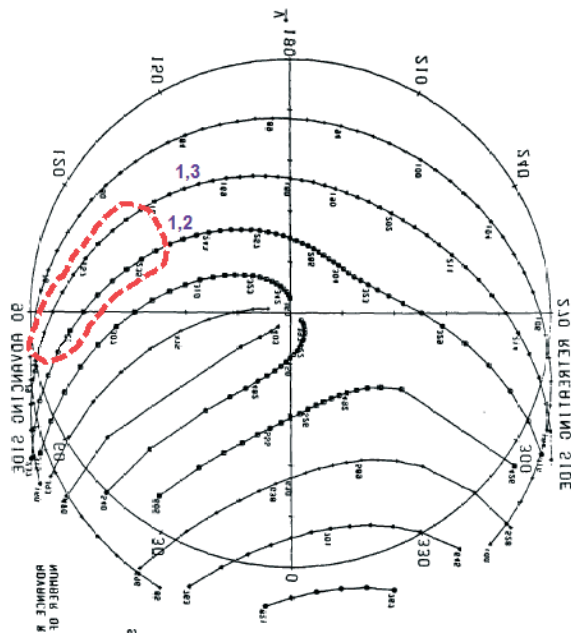


Figure 10: Plot of potential BVI locations and interacting vortices in the acoustically dominant BWI region.

4.2. Statistical and spectral properties of BWI blade pressure fluctuations

For the analysis of blade pressure waveforms the pressure side (lower surface) measurements are employed, as they experience stronger BWI fluctuations compared to the suction side. The strong fluctuations on the pressure side are attributed to the vortex turbulence passing mainly below the rotor disk due to its angle to the free flow. The 0.7R pressure transducer was selected as being in the most active BWI region of the rotor disk containing significant levels of Type II BWI fluctuations. The measured pressure waveform can be seen in Figure 11 (a) and the filtered BVI and BWI components of the advancing side in Figure 11 (b).

In Figure 11 (b) the BWI fluctuations are seen in the region between 85 and 115 deg coinciding with the region of two BVI pulses (1,2 and 1,3). This region is shown in the dotted box, which indicates the bounds of the respective window to be used for the spectral and statistical analysis. Analysing the waveforms from other pressure transducers in the BWI region, it can be observed that Type II pressure fluctuations are found to be located in the region between the two vortices. This observation could strengthen the hypothesis that coherent structures encountered by the blade are formed due to the interaction of co-rotating vortex pairs.

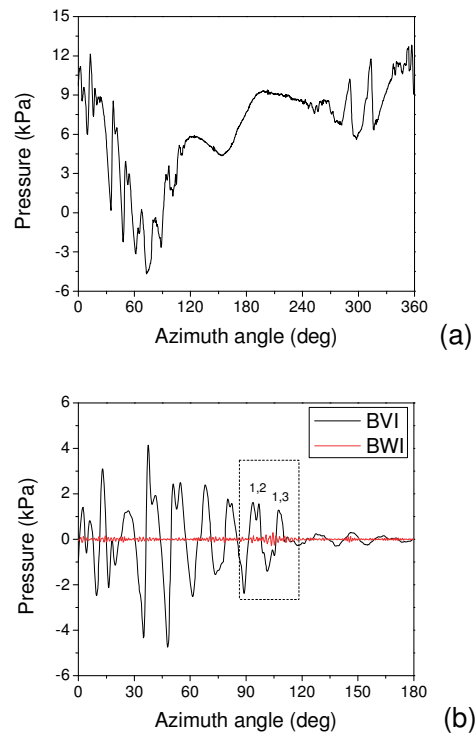


Figure 11: Blade pressure waveform at 2% chord, 0.7R, pressure side (a) and corresponding BVI/BWI filtered signals on the advancing side (b).

The Type II blade pressure fluctuations are then analyzed in a similar way to acoustic fluctuations in terms of probability distribution and spectra properties. Figure 12 (a) shows the statistical distribution to have minor deviations from the Gaussian. Figure 12 (b) shows the average spectrum of Type II fluctuations as a function of Struh number. It can be observed that the maximum occurs around 2.5, similarly to the acoustic fluctuations analysis [Figure 7 (c)]. The slight departure from gaussianity observed in the left part of Figure 12 (a) was also observed in the analysis of BWI pressure fluctuations in take-off conditions made by Bouchet *et al.* It is possible that this departure could be due to BVI high frequency components present in Type II fluctuations.

Regarding Type I pressure fluctuations on the advancing side, they are mainly encountered at 0.95 radius, 50 to 85 deg azimuth, as seen in Figure 9 (c) and in agreement to the localization of the acoustic analysis. These fluctuations do not exhibit a Gaussian distribution, similarly to Type I acoustic fluctuations.

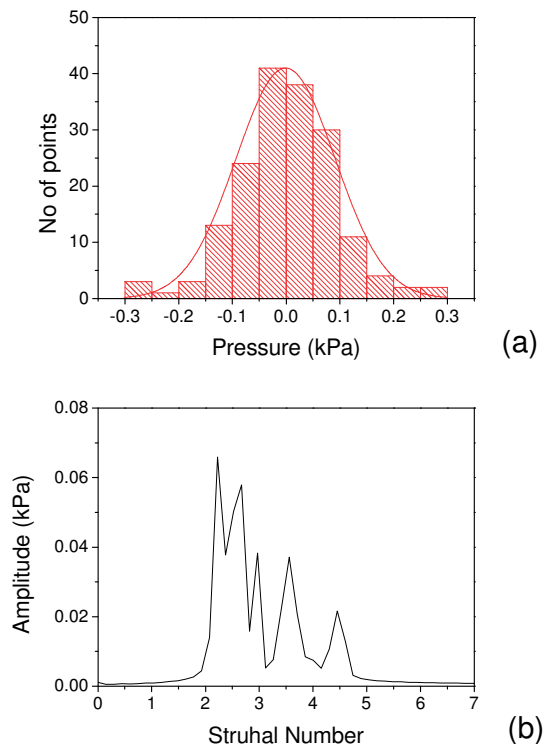


Figure 12: Statistical Distribution of Type II blade pressure fluctuations (a) and their spectrum vs. Struhal Number (b) at 2% chord, $0.7R$, pressure side.

It is concluded that acoustic and aerodynamic BWI fluctuations can be both categorized into two different categories (Type I and Type II) depending on their origin. Type II acoustic and Type II blade pressure fluctuations have similar statistical and spectral properties, which are in agreement with BWI fluctuations' properties resulted from take off conditions' analysis.

The existence of the 2.5 Struhal number agrees and reinforces the suggestion that BWI noise is connected to interaction of the blade to coherent structures present in the rotor's wake. It is observed though, that Type II pressure fluctuations responsible for BWI noise are encountered in the region of two older vortices, while no fluctuations are seen in the region of younger vortices. This could mean that elliptic instabilities are not generated in all co-rotative vortex pairs as younger vortices may not have yet interacted with older vortices to form turbulent coherent structures.

5. EFFECT OF BLADE TIP SHAPE

To the best of the authors' knowledge, the effect of blade tip shape on BWI noise has not been considered before. A similar analysis to the one applied to blade 7A with the rectangular tip has been

applied to blade 7AD that has a swept-back parabolic anhedral tip. The two cases show both similarities and differences.

The Struhal number and probability distribution analysis showed that Type I and II regions are characterized by the same properties for both blade tip cases. The location of the BWI region and of the vortices encountered is the same for both blade tips, showing that blade tip has no significant effect on the turbulence encountered by the blade.

The most important difference between the two cases was seen in the acoustic spectrum data. The BWI frequency region of the average spectra seems to be significantly higher for the rectangular blade tip case [Figure 13(a)]. Comparison of the BWI-filtered acoustic pressure fluctuations of the two blades [Figure 13(b)] shows that this difference is largely attributed to Type I fluctuations, which are of higher amplitude in the rectangular case. This is due to the steeper BVI pulses compared to the swept blade tip case, which amplify the higher frequencies (scallop) of the acoustic spectrum^[17]. Type II fluctuations seem to be the same for the two blades suggesting that there is no difference in acoustic fluctuations originating from blade turbulence interaction.

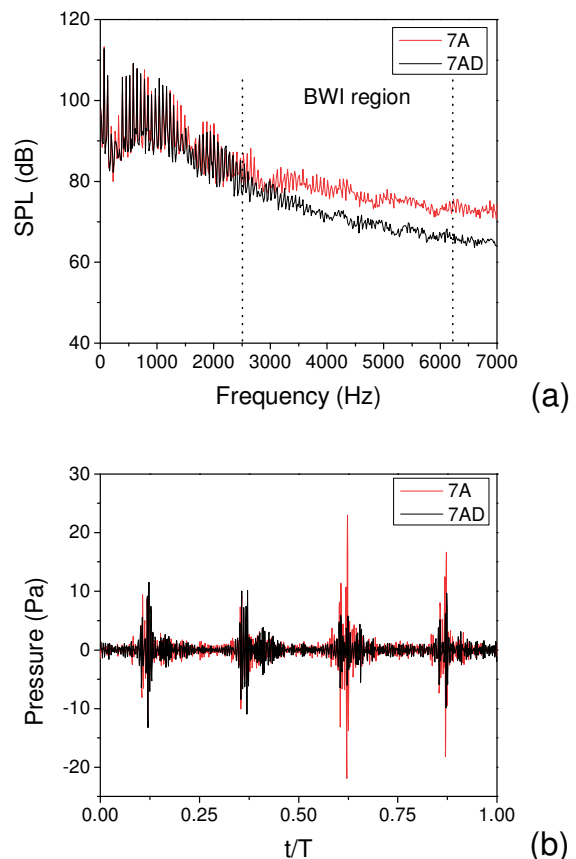


Figure 13: Average spectra (a) and acoustic fluctuations after BWI filtering (b) for the two different blade tips (Mic 3/x=-2).

6. CONCLUSIONS

Acoustic and aerodynamic data from the HELISHAPE experiment have been analyzed to investigate BWI noise in descent flight conditions. Application of appropriate BWI filters to both acoustic and aerodynamic data showed that BWI fluctuations can be divided to Type I and Type II with respect to their origin being impulsive blade vortex interaction or blade turbulence interaction, respectively. Impulsive BVI events come before BWI noise and are not sources of BWI noise, as proposed in the past. Acoustic BWI fluctuation analysis in terms of Struhal number and probability distribution was found to be in agreement with the aerodynamic data analysis and with similar previous analysis on take-off flight conditions. The results can be further considered as providing support to the theory that connects BWI noise to elliptic instabilities of co-rotating vortices. The acoustically dominant BWI region was located to be between $0.85R$ at 85° and $0.62R$ at 115° azimuth. Use of wake charts provided the vortices encountered in that region showing that BWI fluctuations do not come in the region of younger vortices, possibly, because no elliptic instabilities have yet formed. Finally, it was found that the blade tip can affect the Type I fluctuations, but does not affect Type II, which are the fluctuations attributed to blade wake interaction.

ACKNOWLEDGEMENTS

The work has been partially supported by the European Integrated Project FRIENDCOPTER.

REFERENCES

- [1] Y. H. Yu, "Rotor blade-vortex interaction noise," *Progress in Aerospace Sciences* 36, 97-115 (2000).
- [2] F. H. Schmitz, Rotor noise, NASA Ames Research Center, Moffett Field, California, 1991.
- [3] T. F. Brooks, J. R. Jolly, M. A. Marcolini, "Helicopter Main Rotor Noise: Determination of Source Contributions using Scaled Model Data", NASA Technical Paper 2825, August 1988.
- [4] S. A. L. Glegg, "Prediction of Blade Wake Interaction Noise Based on a Turbulent Vortex Model", *AIAA Journal*, Vol. 29 (10), 1991.
- [5] K. S. Wittmer, W. J. Devenport, S. A. L. Glegg, "Perpendicular Blade Vortex Interaction", *AIAA Journal*, Sept 1995, pp 1667-1674.
- [6] S. A. L. Glegg, S. Wittmer, J. Devenport, D. S. Pope, "Broadband Helicopter Noise", AHS Specialists' Meeting for Rotorcraft Acoustics and Aerodynamics, Williamsburg, Virginia, Oct 1997.
- [7] J. Brezillion, J. Prieur, J. Rahier, "Investigation on Broadband Helicopter Noise", AHS Rotorcraft Acoustics and Aerodynamics Specialists Meeting, Williamsburg, Virginia, Oct 1997.
- [8] W. R. Spletstoesser, R. Cube, W. Wagner, U. Seelhorst, A. Boutier, F. Micheli, E. Mercker, K. Pengel, "Key results from a Higher Harmonic Control Aeroacoustic Rotor Test (HART)", *Journal of the AHS*, 1997, 42(1).
- [9] E. Bouchet, G. Rahier, "Structure of the Blade Pressure Fluctuations Generated by Helicopter Rotor Blade-Wake Interaction", 56th AHS Annual Forum, Virginia Beach, Virginia, May 2000.
- [10] W. J. Devenport, C. M. Vogel, J. S. Zsoldos, "Flow structure produced by the interaction and merger of a pair of co-rotating wing-tip vortices", *J. Fluid Mech*, vol 394, pp. 357-377, 1999.
- [11] K. J. Schultz, W. Spletstoesser, B. Junker, W. Wagner, "A parametric windtunnel test on rotorcraft aerodynamics and aeroacoustics (HELISHAPE) – test procedures and representative results," 22nd European Rotorcraft Forum, Brighton, UK, 1996.
- [12] Y. Mauffrey, G. Rahier, J. Prieur, "Numerical Investigation on Blade-Wake Interaction noise. Towards a better understanding of BWI mechanisms", 32nd European Rotorcraft Forum, Maastricht, The Netherlands, September 2006.
- [13] O. Schneider, B.G. van der Wall, "Comparison of Simple and Conditional Averaging Methodology Based on Results of the HART II Wind Tunnel Test", International Forum on Rotorcraft Multidisciplinary Technology, Seoul, Korea, (2007).
- [14] M. A. Marcolini, T. F. Brooks, "Rotor Noise Measurement Using a Directional Microphone Array", *AIAA Paper* 87-2746, 1987.
- [15] W. R. Spletstoesser, K. J. Schultz, and R. M. Martin. "Rotor Blade-Vortex Interaction Impulsive noise Source localization", *AIAA Journal*, Vol. 28, 593-600, April 1990.
- [16] T. A. Egolf and A. J. Landgrebe, "Helicopter Rotor Wake Geometry and its Influence in Forward Flight, Volume II – Wake Geometry Charts", NASA CR 3727, 1983.
- [17] R. M. Martin. J. C. Hardin, "Spectral Characteristics of Rotor Blade/Vortex Interaction Noise", *J. Aircraft*, Vol.25, No. 1, 1987.